Dual Pseudo-Isothermal Ellipsoid (dPIE)

Includes both core and truncation radius making it both non-singular and finite mass.

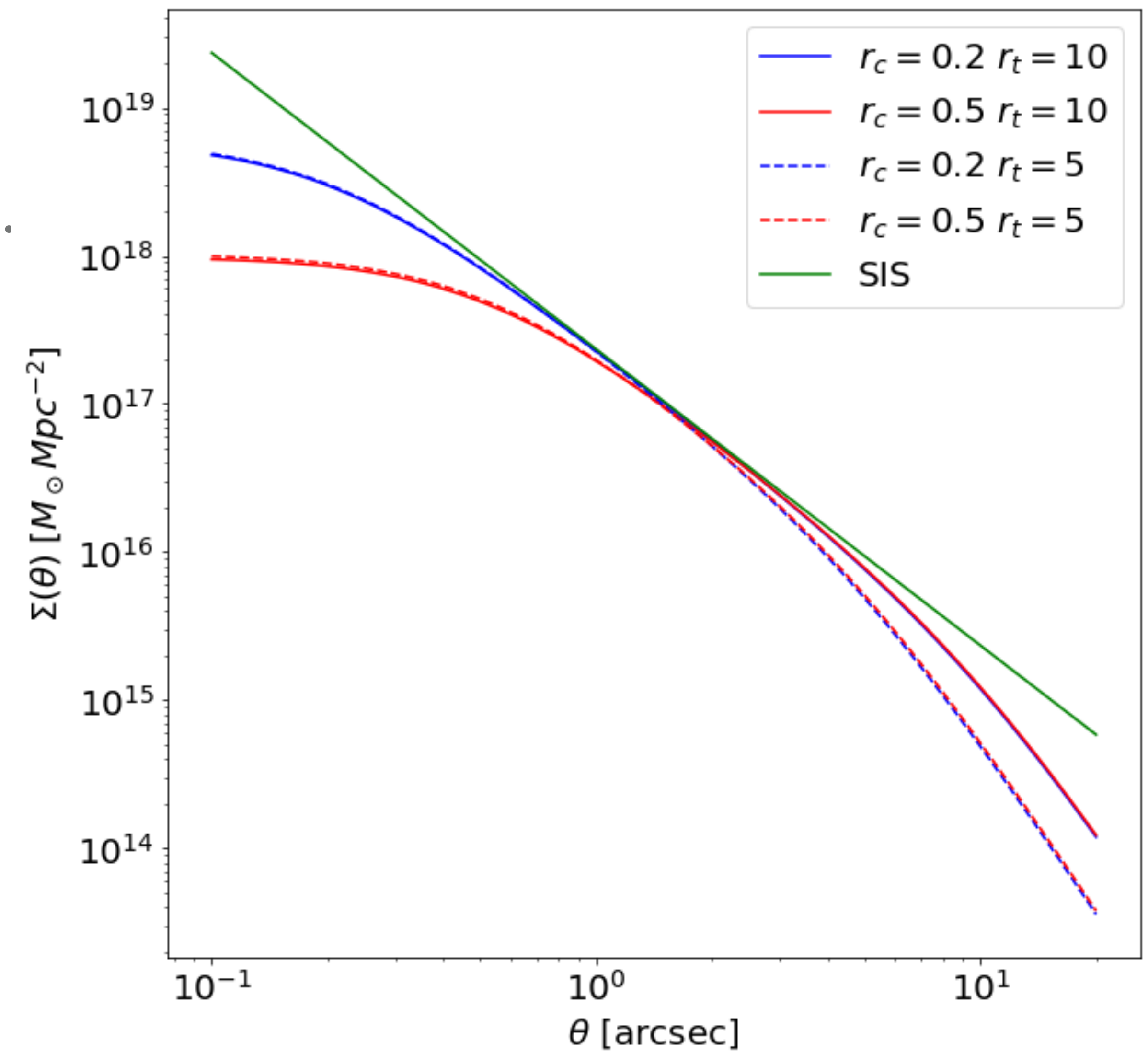

$$\rho(r) = \frac{\rho_0}{\left(1 + \frac{r^2}{r_c^2}\right)\left(1 + \frac{r^2}{r_t^2}\right)}$$

$$\rho_0 = \frac{\sigma_0^2}{2\pi G}\frac{r_c + r_t}{r_c^2 r_t} \qquad r_t > r_c$$

The surface density is

$$\Sigma(\xi) = \frac{\sigma_0^2}{2G}\frac{r_t}{r_t - r_c}\left(\frac{1}{\sqrt{\xi^2 + r_c^2}} - \frac{1}{\sqrt{\xi^2 + r_t^2}}\right)$$

Thus the dPIE is equivalent to two non-singular isothermal spheres (NSIE), one having negative mass and canceling the other out at distances >> r_t.

PARAMETRIC LENS MODELLING

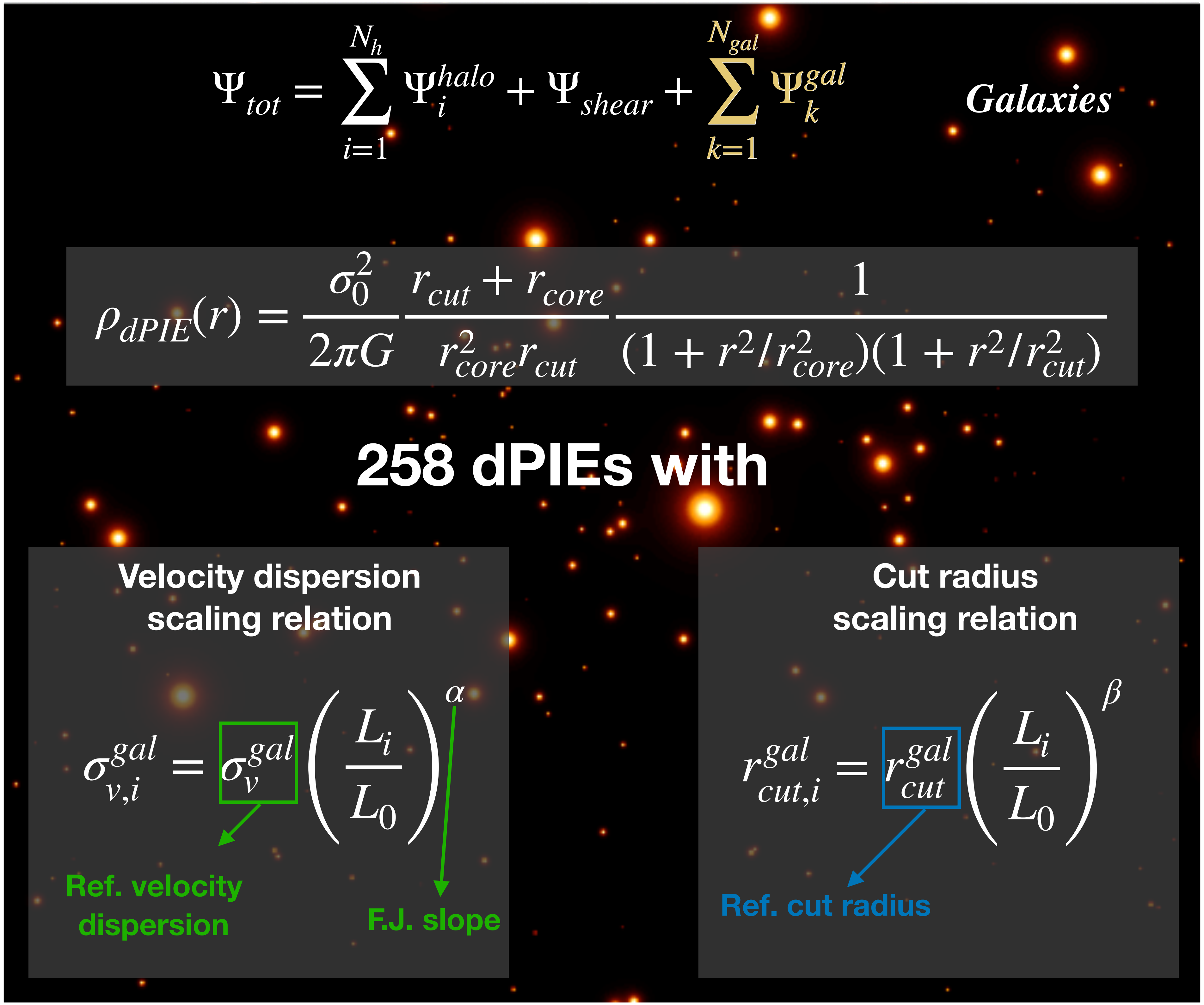

$$\Psi_{tot} = \sum_{i=1}^{N_h} \Psi_i^{halo} + \Psi_{shear} + \sum_{k=1}^{N_{gal}} \Psi_k^{gal}$$

Galaxies

$$\rho_{dPIE}(r) = \frac{\sigma_0^2}{2\pi G} \frac{r_{cut} + r_{core}}{r_{core}^2 r_{cut}} \frac{1}{(1 + r^2/r_{core}^2)(1 + r^2/r_{cut}^2)}$$

258 dPIEs with

Velocity dispersion scaling relation

$$\sigma_{v,i}^{gal} = \boxed{\sigma_v^{gal}} \left(\frac{L_i}{L_0} \right)^{\alpha}$$

Ref. velocity dispersion

F.J. slope

Cut radius scaling relation

$$r_{cut,i}^{gal} = \boxed{r_{cut}^{gal}} \left(\frac{L_i}{L_0} \right)^{\beta}$$

Ref. cut radius

MACSJ1206 @z=0.439 (Bergamini et al. 2019, Bonamigo et al. 2018, Caminha et al 2017)

PARAMETRIC LENS MODELLING

$$\chi^2(\vec{\mathbf{p}}) = \sum_{j=1}^{N_{fam}} \sum_{i=1}^{N_{im}} \left(\frac{[\vec{\theta}_{i,j} - \vec{\theta}'_{i,j}(\vec{\mathbf{p}})]}{\Delta x_{i,j}} \right)^2$$

$$N_{im} = 82 \qquad N_{fam} = 27$$

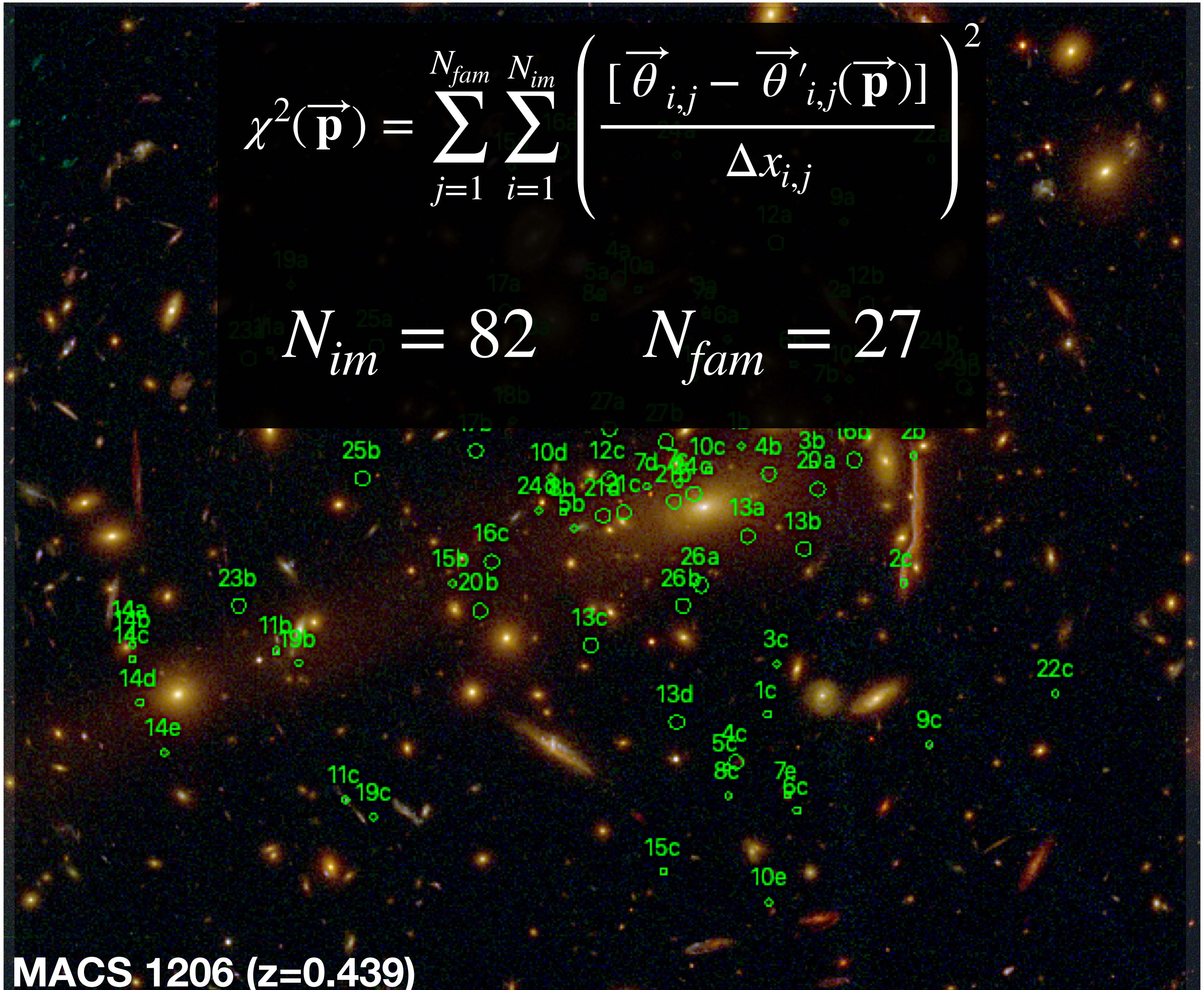

MODEL OF MACSJ1206 (CAMINHA ET AL. 2017)

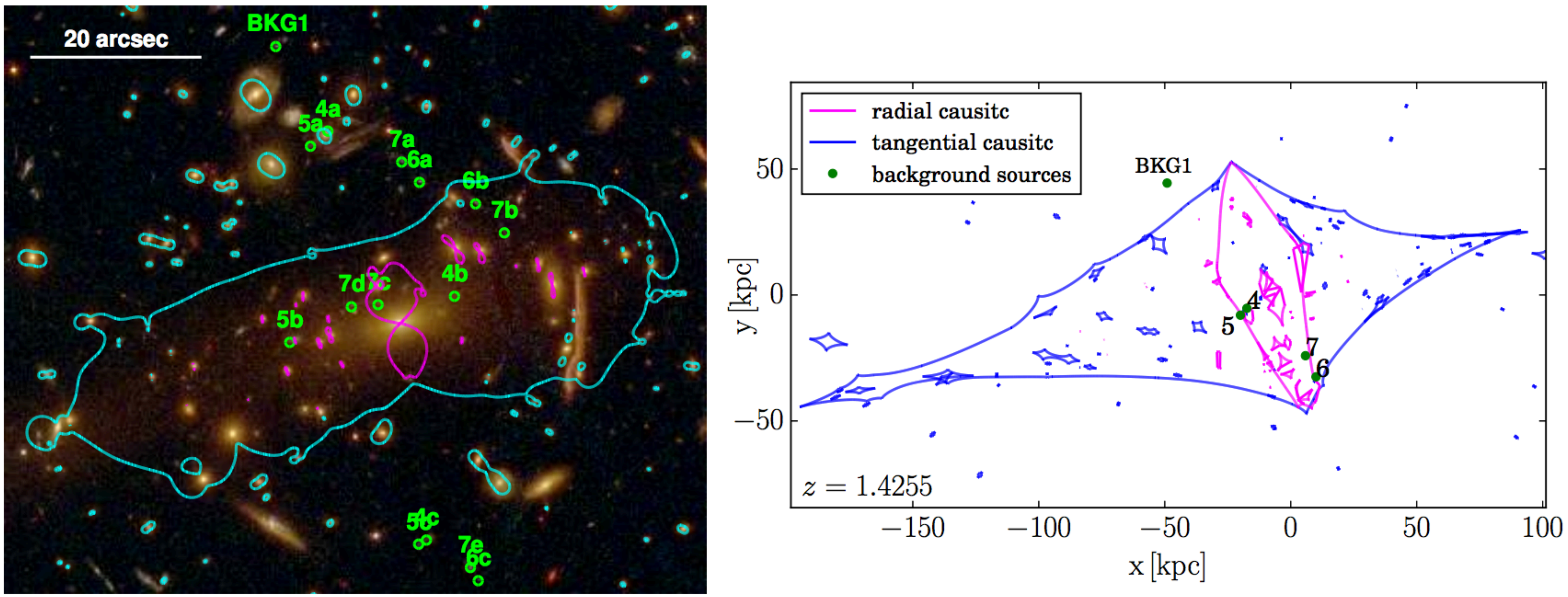

Fig. 6: Critical curves and caustics of the reference model P3ε for a source at $z_{src} = 1.4255$ (the mean redshift values of the sources). Left panel: Tangential (cyan) and radial (magenta) critical lines on the image plane. The green circles show the observed positions of the multiple images belonging to the four families within $\Delta z \leq 0.0011$. BKG1 is a background galaxy not multiply lensed by MACS 1206. Right panel: Tangential (cyan) and radial (magenta) caustics on the source plane, and the reconstructed positions of the background sources.

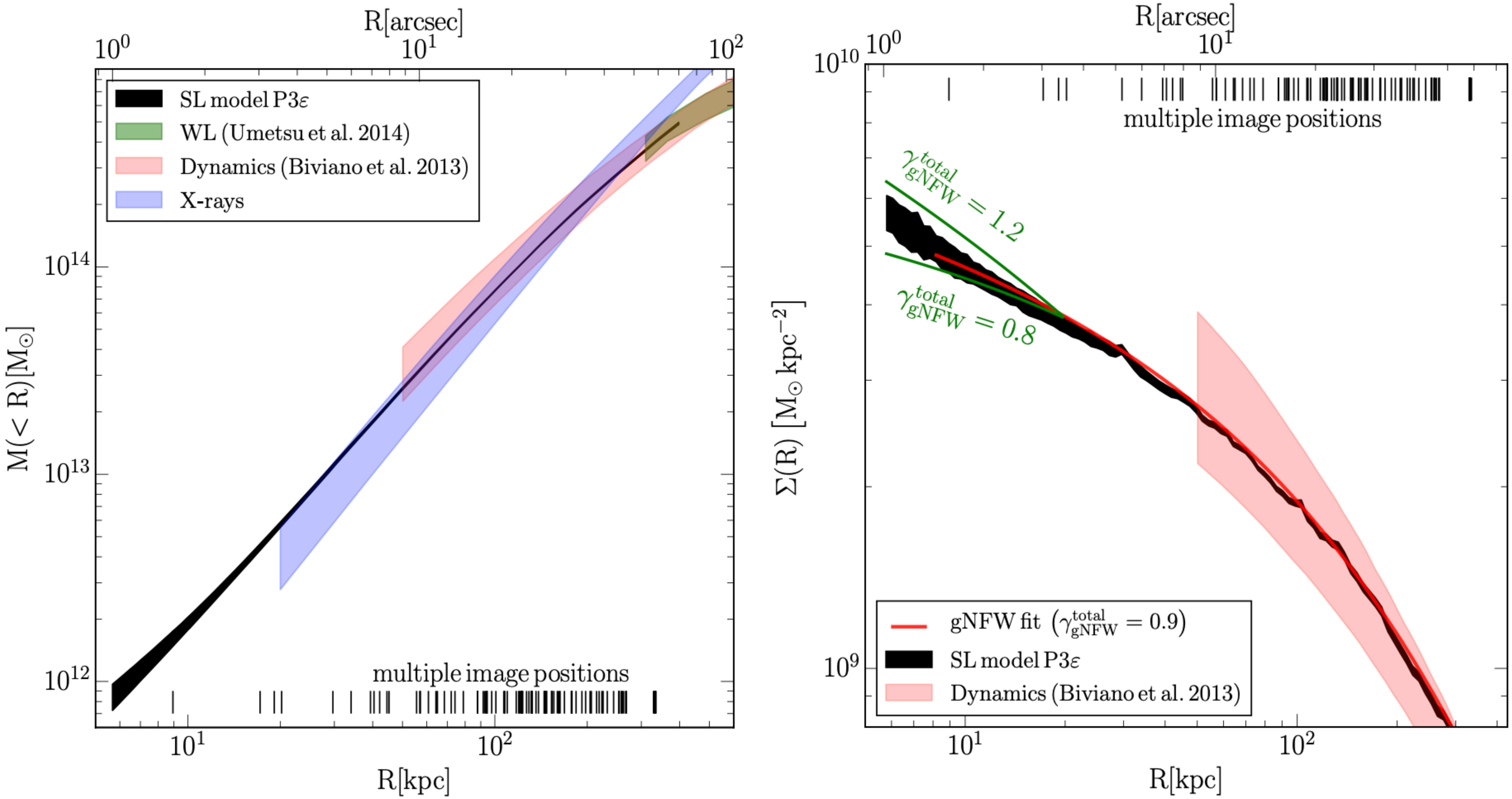

Fig. 7: Comparison of different independent projected total mass determinations in MACS 1206. The black region represents the results at the 95% confidence level of our strong lensing analysis (reference model P3ε). At the 68% confidence level, the dynamical (Biviano et al. 2013), weak-lensing (Umetsu et al. 2014), and X-ray (see Sect. 4.2) total mass estimates are shown in red, green, and blue, respectively. The vertical lines indicate the projected radial distances from the cluster center of the multiple images presented in this work. The cumulative projected total mass profile is shown in the left panel. In the right panel we show the projected total surface mass density profile and the red line is a fit using a gNFW model. The green lines show two different gNFW profiles, with values of $\gamma^{\rm total}_{\rm gNFW}$ equal to 0.8 and 1.2, normalized at R = 20 kpc.

MULTIPLE LENS PLANES

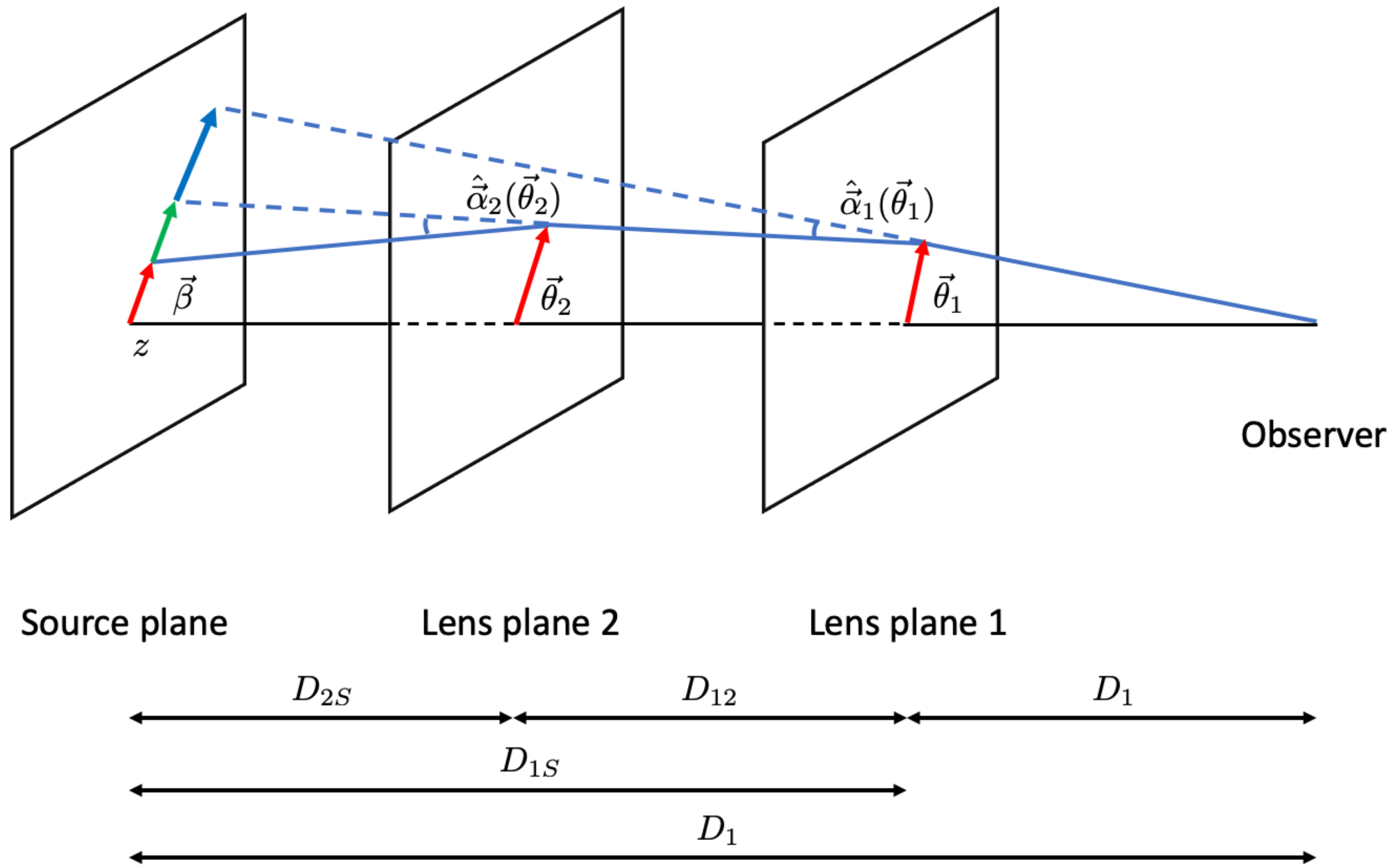

$$D_S \vec{\beta} = D_S \vec{\theta}_1 - D_{1S} \hat{\vec{\alpha}}_1(\vec{\theta}_1) - D_{2S} \hat{\vec{\alpha}}_2(\vec{\theta}_2) \qquad \vec{\beta} = \vec{\theta}_1 - \sum_{i=1}^{2} \vec{\alpha}_i(\vec{\theta}_i)$$

$$\vec{\theta}_2 = \vec{\theta}_1 - \frac{D_{12}}{D_2} \hat{\vec{\alpha}}_1(\vec{\theta}_1) = \vec{\theta}_1 - \frac{D_{12}}{D_2} \frac{D_S}{D_{1S}} \vec{\alpha}_1(\vec{\theta}_1)$$

MULTIPLE LENS PLANES

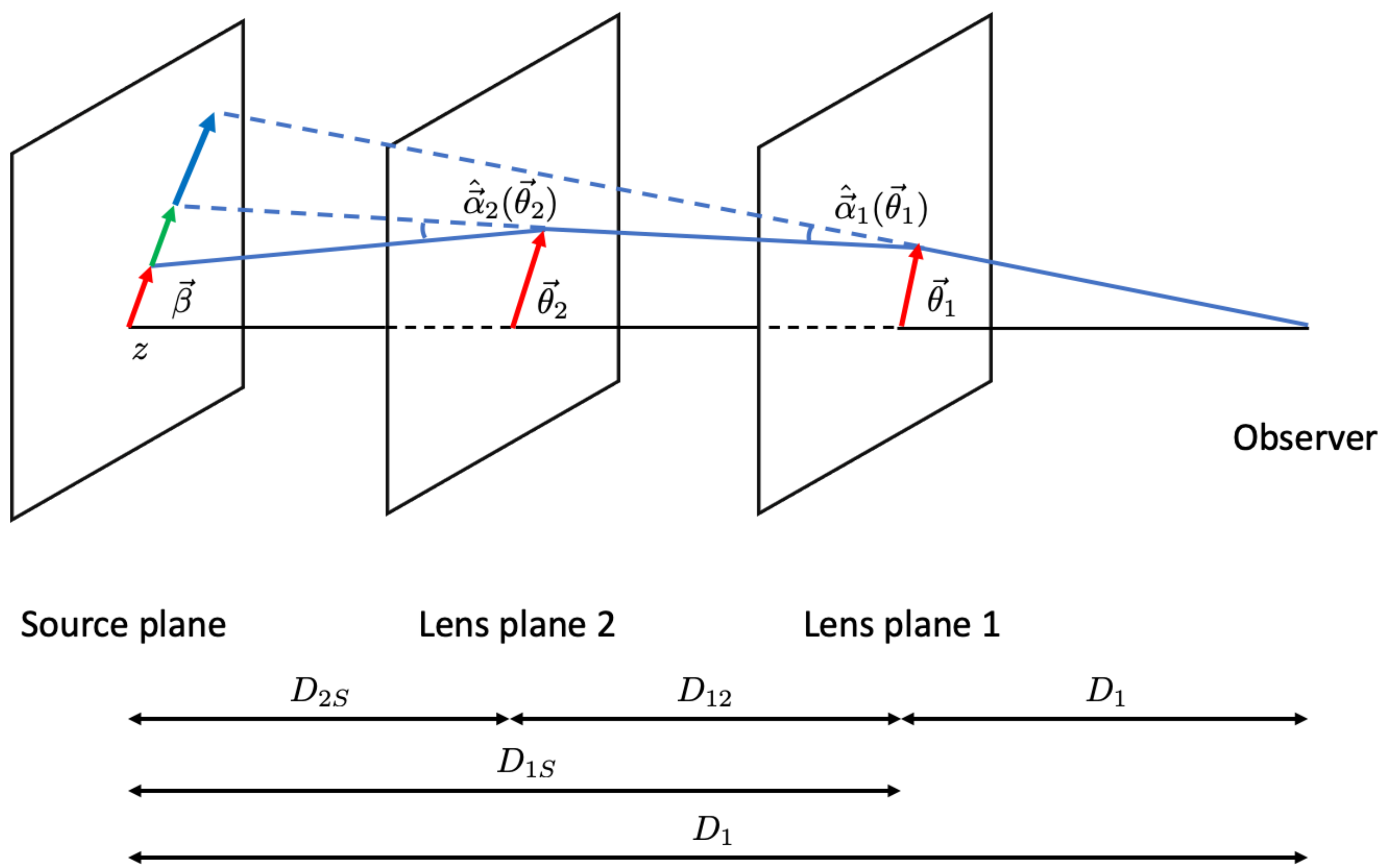

$$\overrightarrow{\beta} = \overrightarrow{\theta}_1 - \sum_{i=1}^{N} \overrightarrow{\alpha}_i(\overrightarrow{\theta}_i)$$

$$\overrightarrow{\theta}_i = \overrightarrow{\theta}_1 - \sum_{j=1}^{i-1} \frac{D_{ji}}{D_i}\frac{D_S}{D_{jS}}\overrightarrow{\alpha}_j(\overrightarrow{\theta}_j)$$

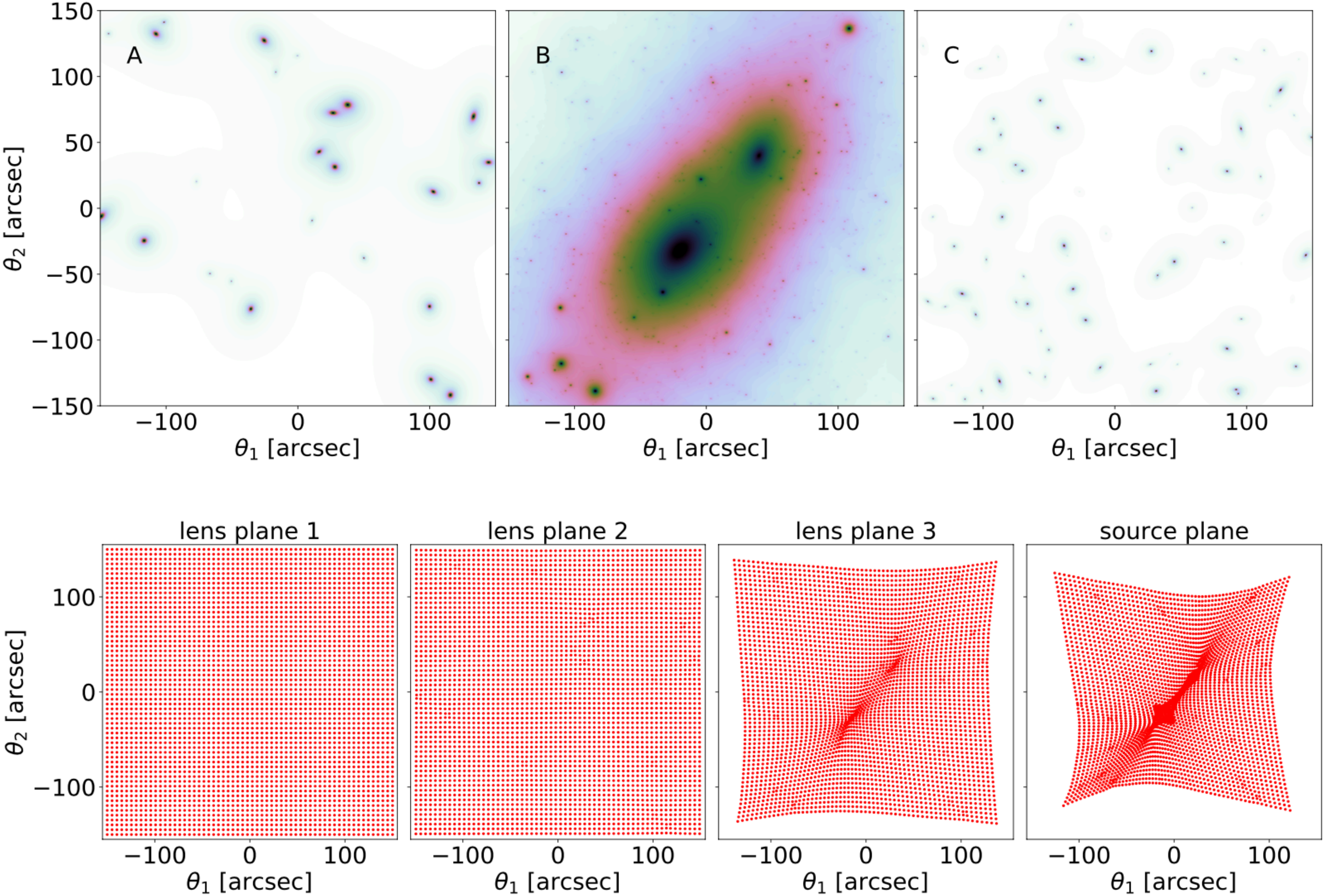

A
B
C
θ1 [arcsec]
θ2 [arcsec]
lens plane 1
lens plane 2
lens plane 3
source plane

EXAMPLE

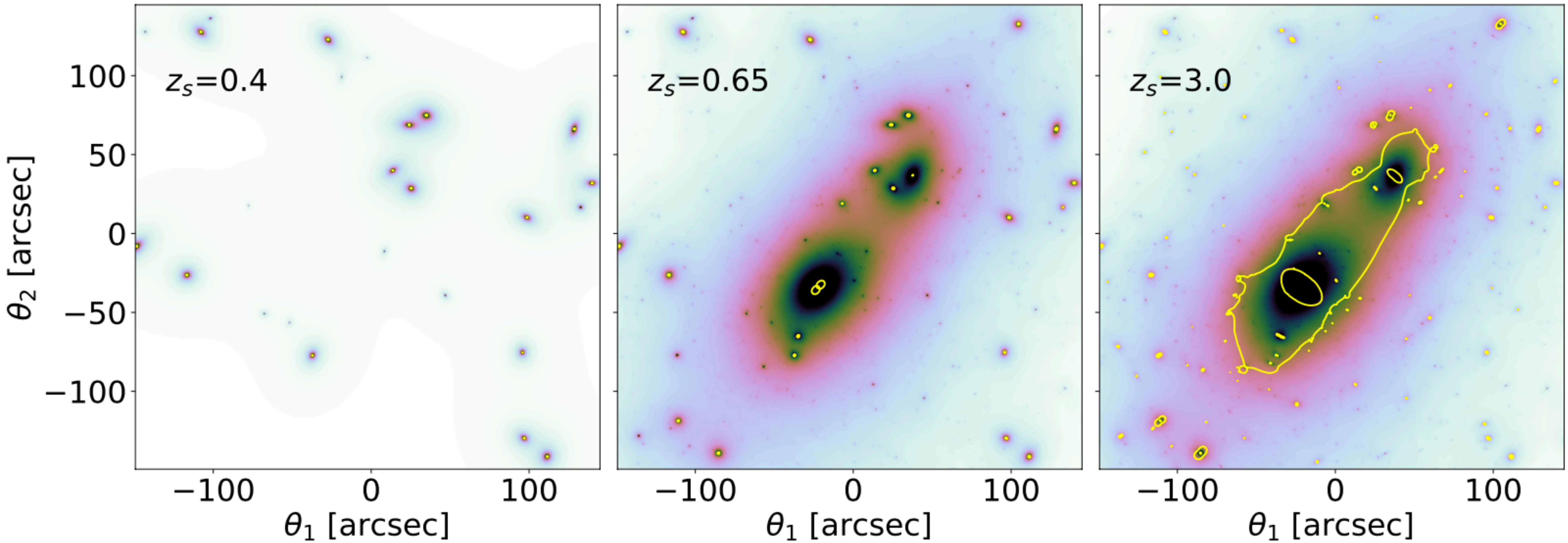

z_s=0.4
z_s=0.65
z_s=3.0
100
50
0
−50
−100
θ_2 [arcsec]
−100
0
100
θ_1 [arcsec]
−100
0
100
θ_1 [arcsec]
−100
0
100
θ_1 [arcsec]

EXAMPLE

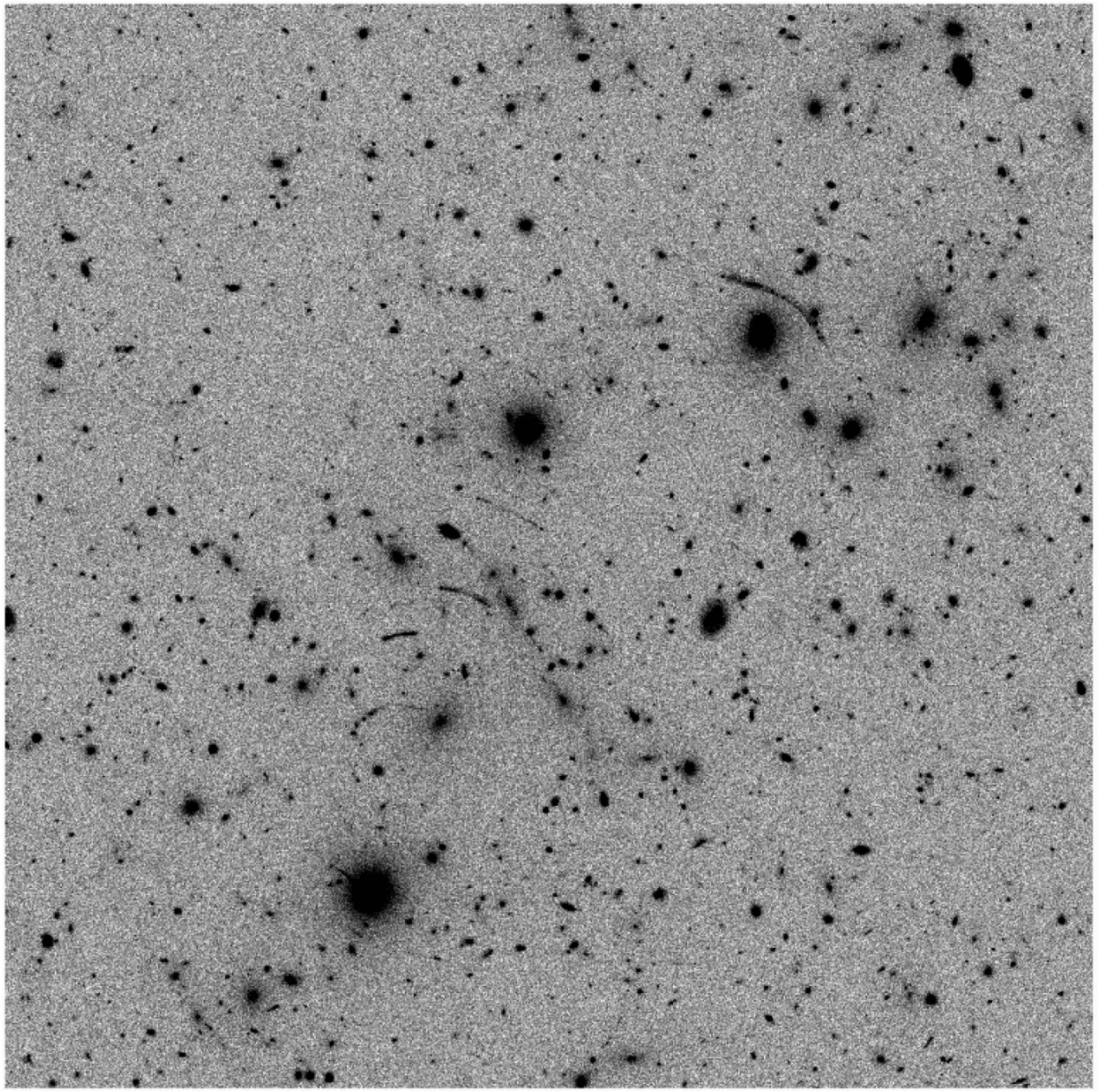

Without LOS

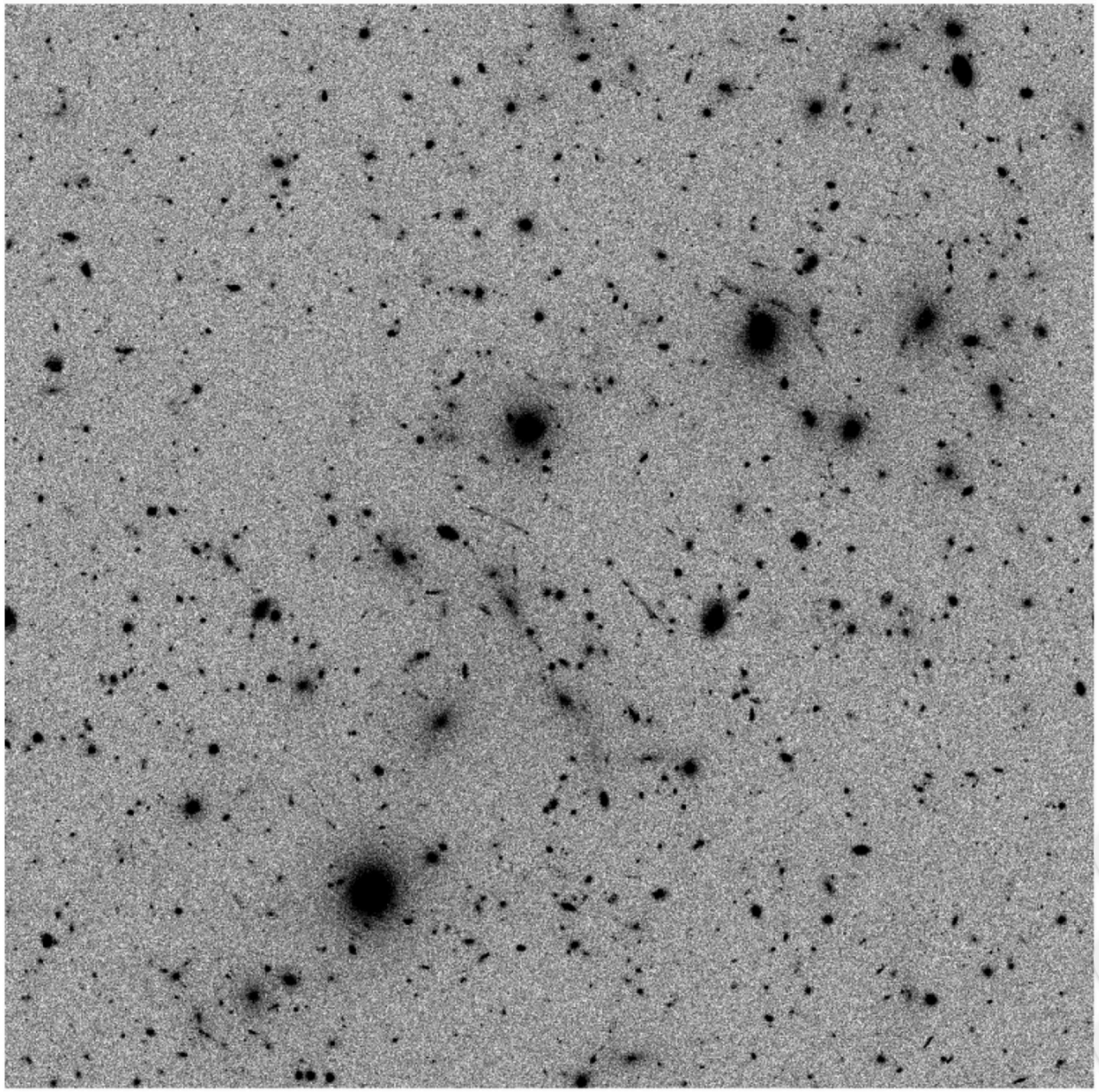

With LOS

FREE FORM SOURCE AND LENS RECONSTRUCTION

In some lenses the source does not have obvious points of light that are multiply imaged, but instead is a continuous smooth surface brightness. This is particularly true in galaxy-galaxy lenses.

Even when there are some points that can be identified the smooth parts might provide additional information about the lens. An example of this is searching for substructure by their distortion of arcs and rings.

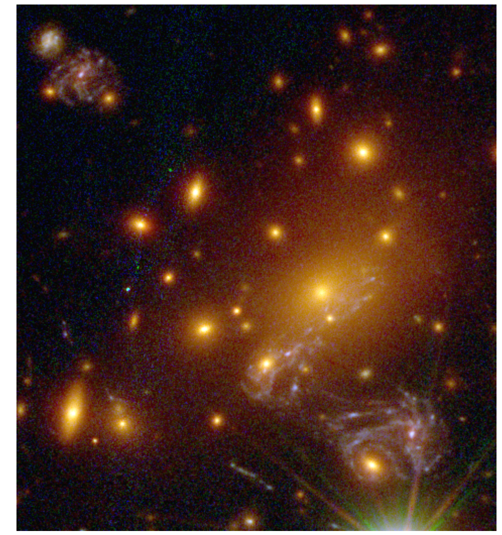

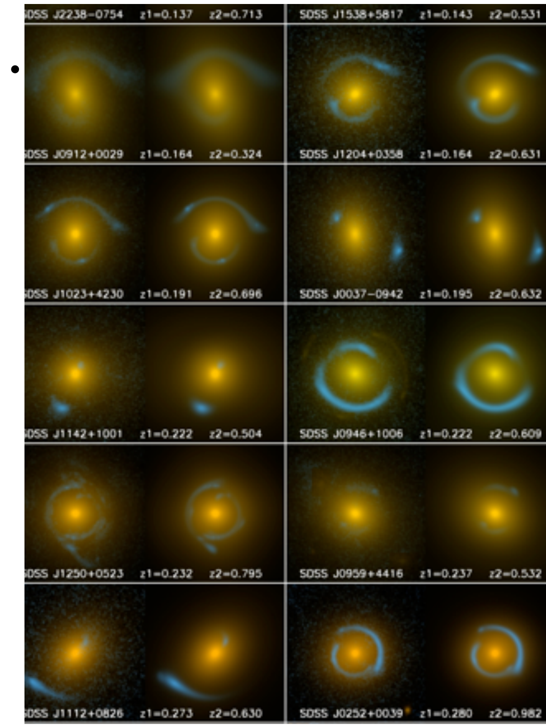

The source and the lens are parameterised. The source model consists of "pixels" that each have a flux.

An image is constructed by shooting rays from the observed pixels to the source pixels.

The chi-squared is calculated from the residuals between the observed pixel values and the predicted ones.

$$\chi^2(\boldsymbol{p}) = \sum_i^{\text{pixels}} \frac{[f_i - f_i(\boldsymbol{p})]^2}{\sigma_f^2}$$

$\boldsymbol{p}$ *- Parameters of lens model & source model*

f_i *- flux in the ith pixel*

FREE FORM SOURCE AND LENS RECONSTRUCTION

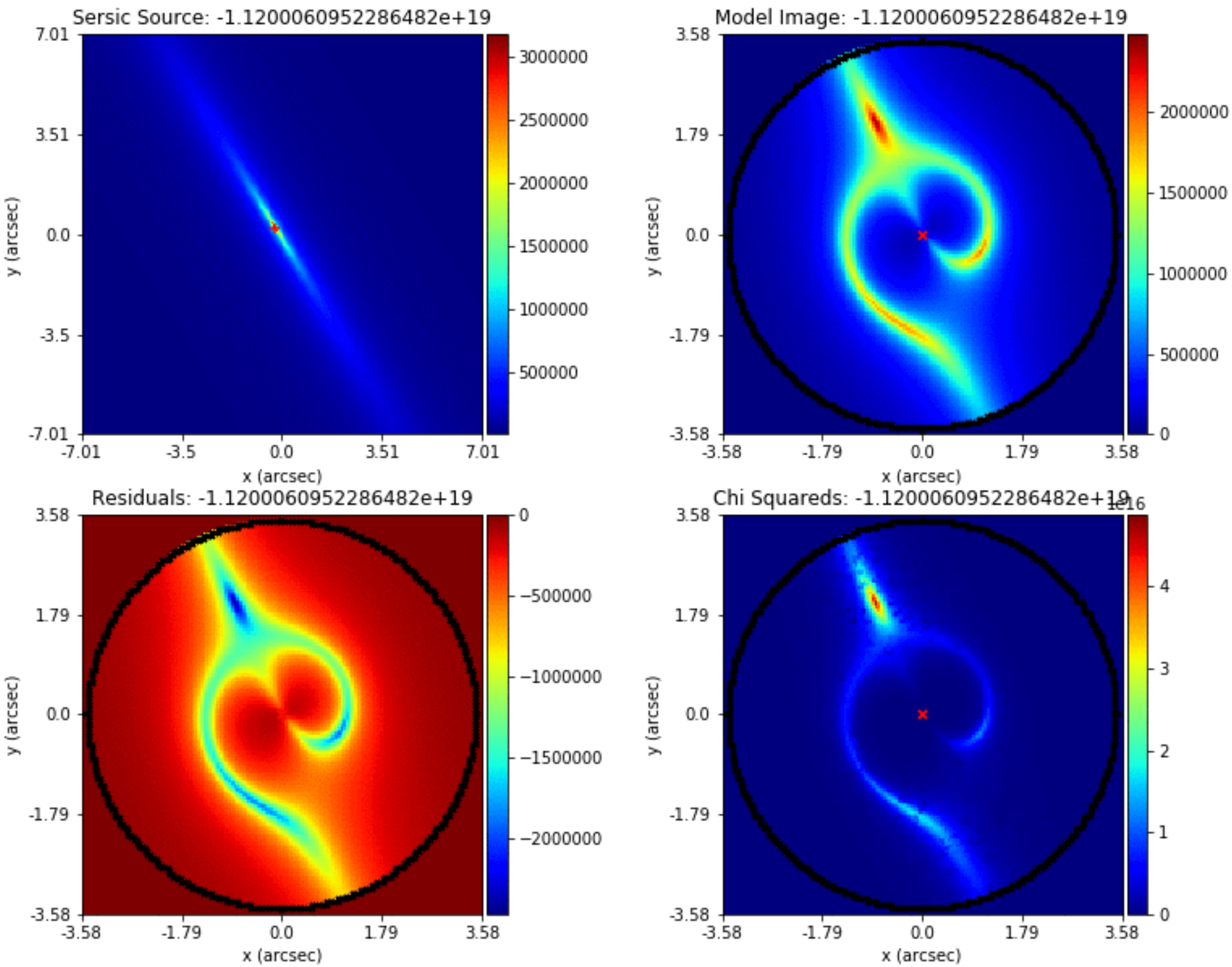

PyAuroLens
reconstruction

FREE FORM SOURCE AND LENS RECONSTRUCTION

pixelation of the source plane

PyAuroLens
reconstruction

uniform square pixelation

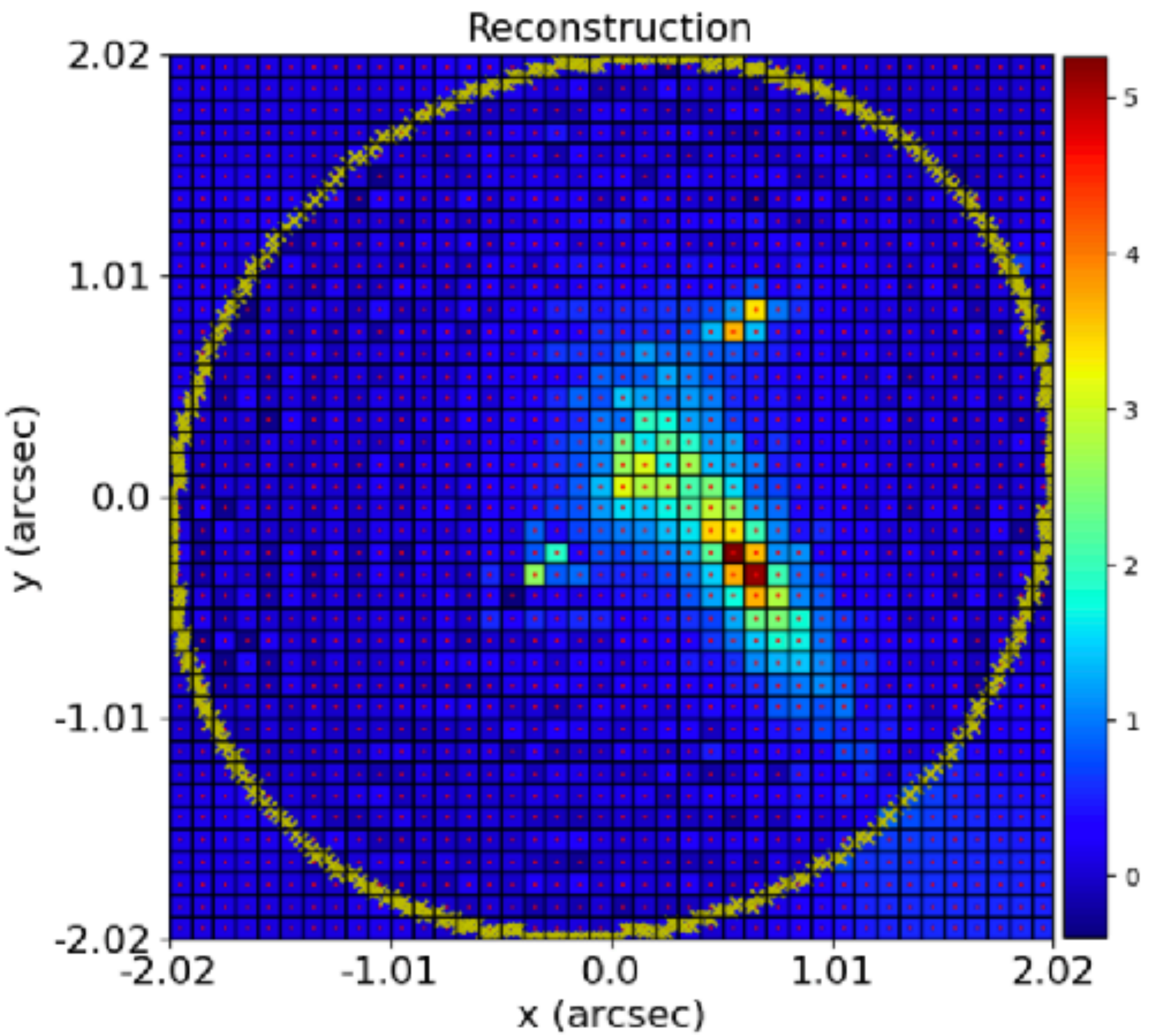

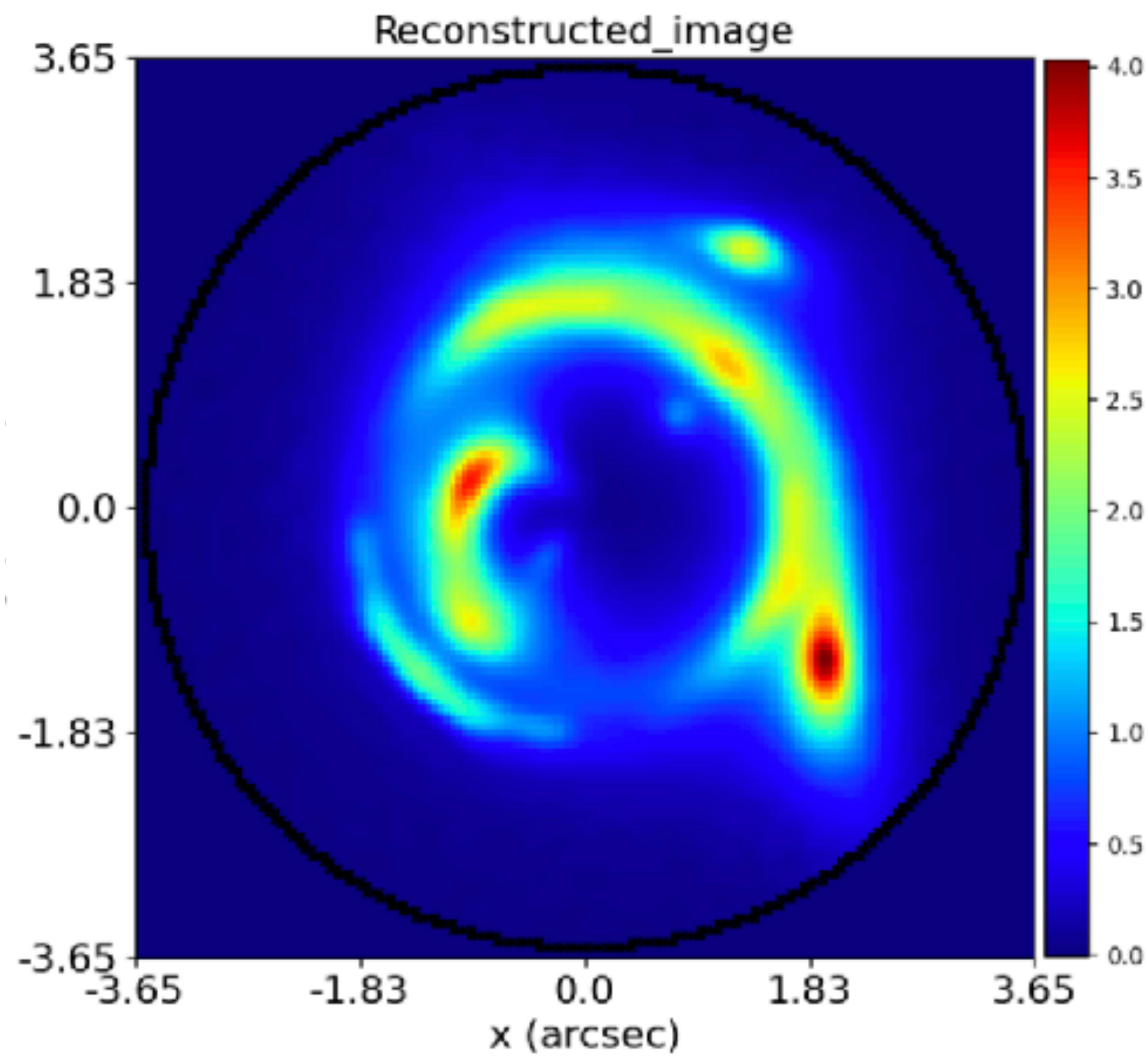

FREE FORM SOURCE AND LENS RECONSTRUCTION

PyAuroLens

reconstruction

pixelation of the source plane

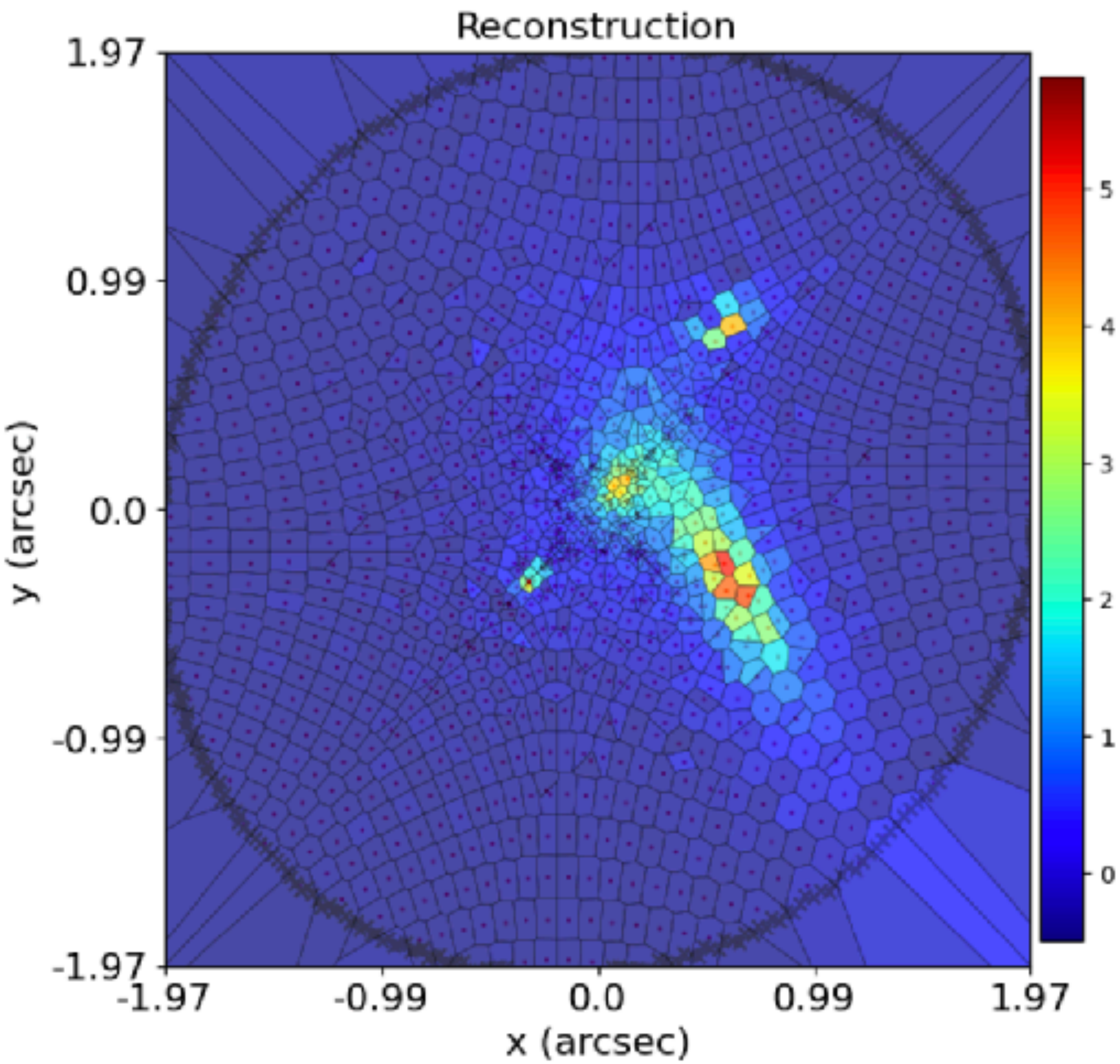

Other pixelations are possible.

Voronoi pixilation of the source plane.

Evenly spaced points on the image plane are shot back to the source plane.

Each cell consists of the region that is closer to the point than any other.

In this way the cells are smaller where the magnification is larger and pixelation adapts to the lens model.

The flux in each of the cells is a parameter

FREE FORM SOURCE AND LENS RECONSTRUCTION

Difficulties:

There are many parameters making finding the best fit solution and exploring the posterior very difficult. This generally limits the method to small lenses like galaxy-galaxy lenses.

There are generally more parameters than observables. This makes the problem ***underdetermined*** *which means that no unique solution can be found without imposing some regularisation or prior on the source. This is generally not well physically motivated.*

> *The regularisation imposes some kind of smoothness on the source's surface brightness. For example, the finite difference curvature of the surface brightness is forced to be small.*
>
> *This comes in the form of a penalty function that is added to the chi squared. There are additional parameters that regulate the strength of the regularisation*

The result will in general depend on the regularisation that is used.

DELAUNAY TESSELLATION

Tessellation of image plane.

Divide image plane into triangles.

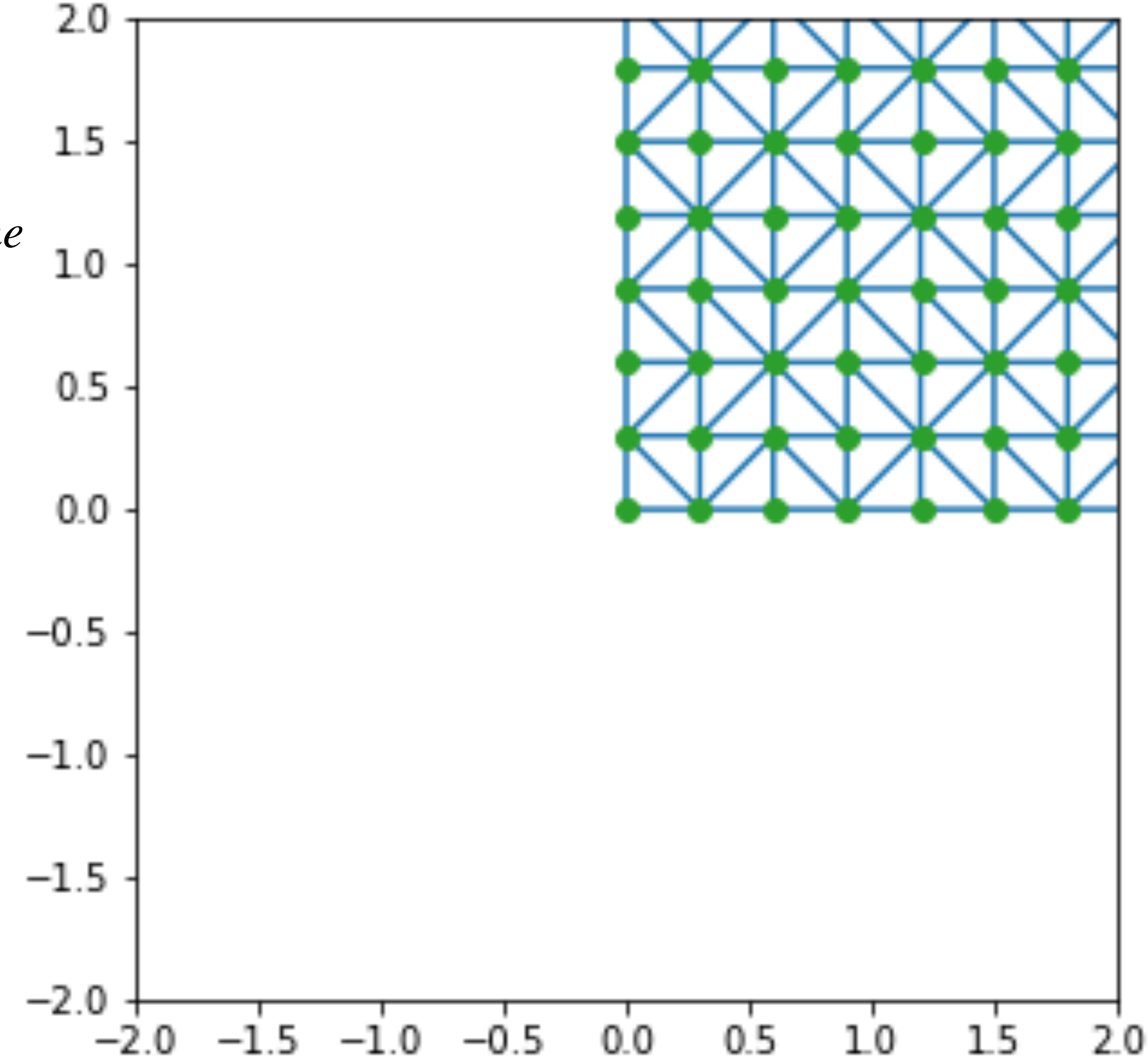

DELAUNAY TESSELLATION

Tessellation of image plane.

Divide image plane into triangles.

Find the source position of each vertex point by adding the deflection.

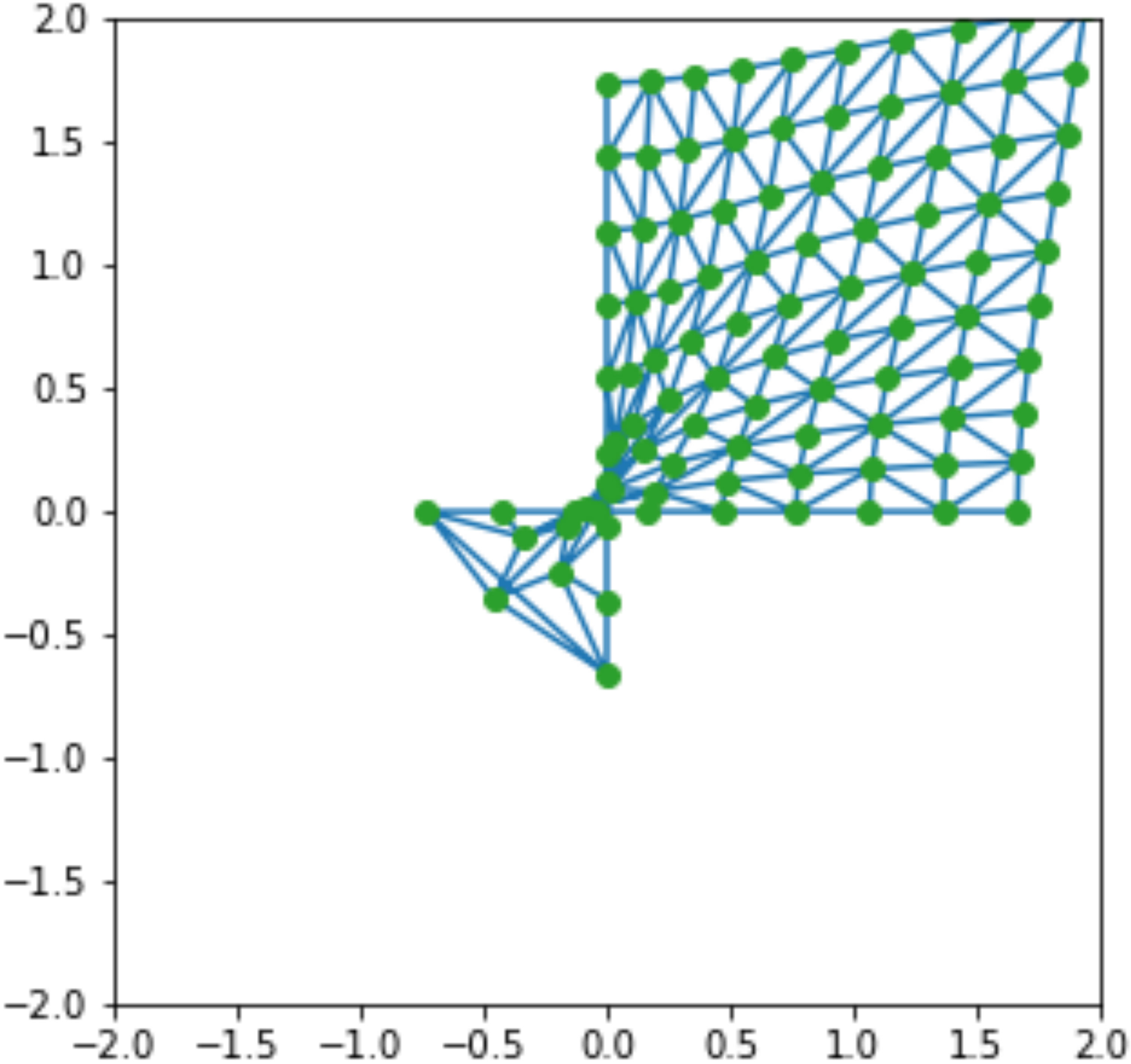

DELAUNAY TESSELLATION

Tessellation of image plane.

Divide image plane into triangles.

Find the source position of each vertex point by adding the deflection.

Find which triangle the source is in.

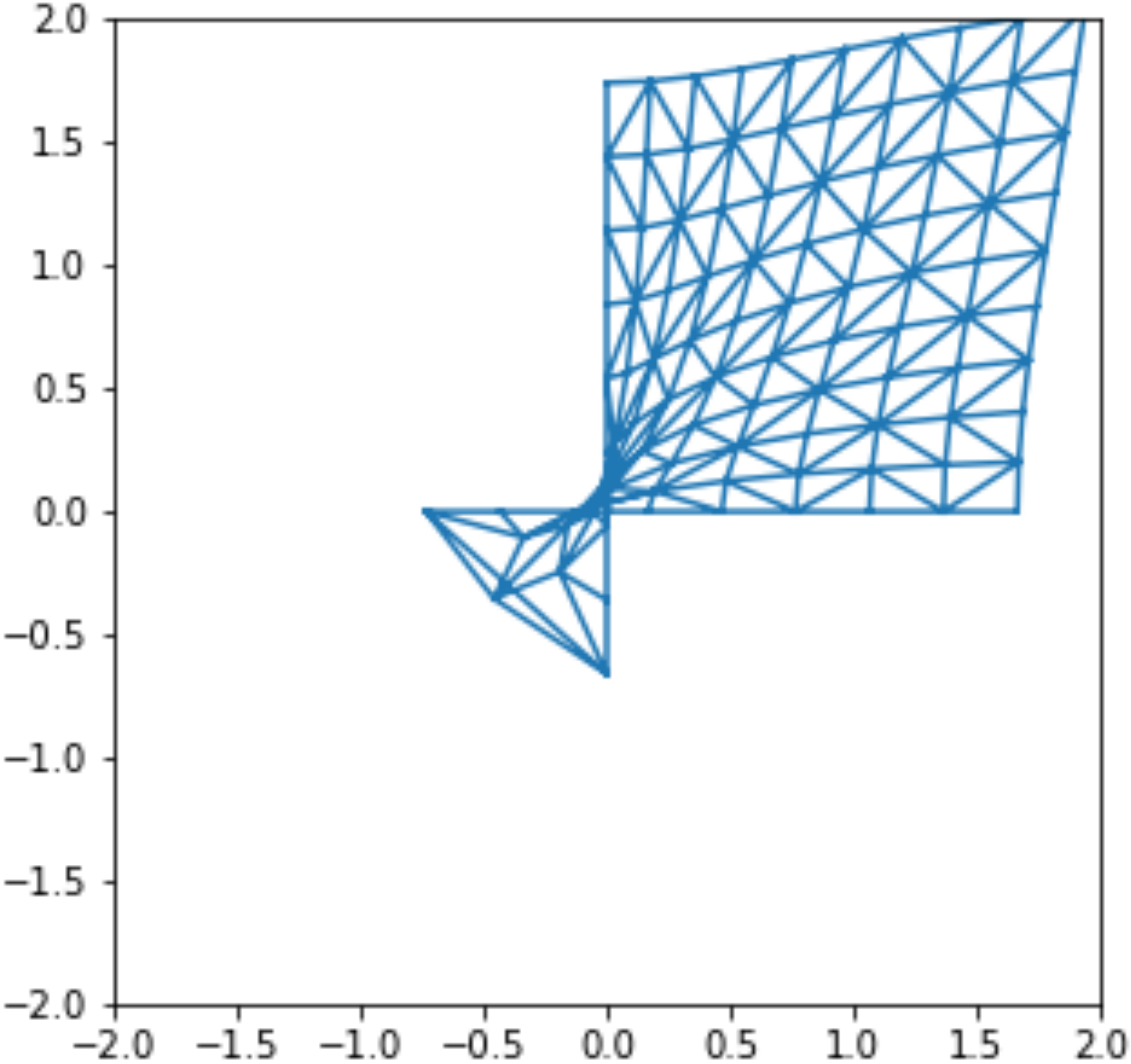

DELAUNAY TESSELLATION

Tessellation of image plane.

Divide image plane into triangles.

Find the source position of each vertex point by adding the deflection.

Find which triangle the source is in.

Since the triangle will overlap, the source will be in more than one triangle.

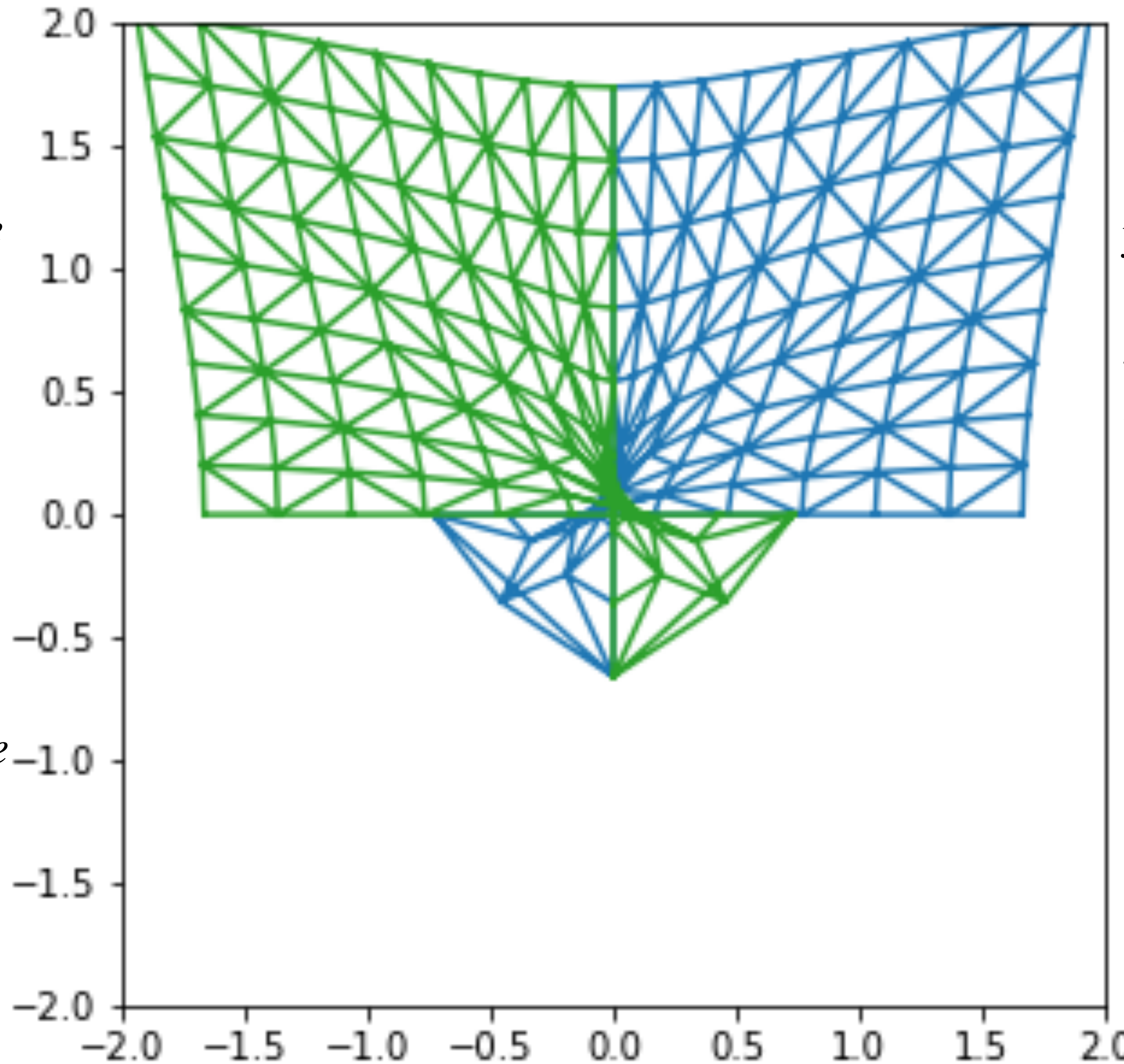

Going back to the triangle on the image plane will tell you where the images are, to the resolution of the tessellation.

DELAUNAY TESSELLATION

Tessellation of image plane.

Divide image plane into triangles.

Find the source position of each vertex point by adding the deflection.

Find which triangle the source is in.

Since the triangle will overlap, the source will be in more than one triangle.

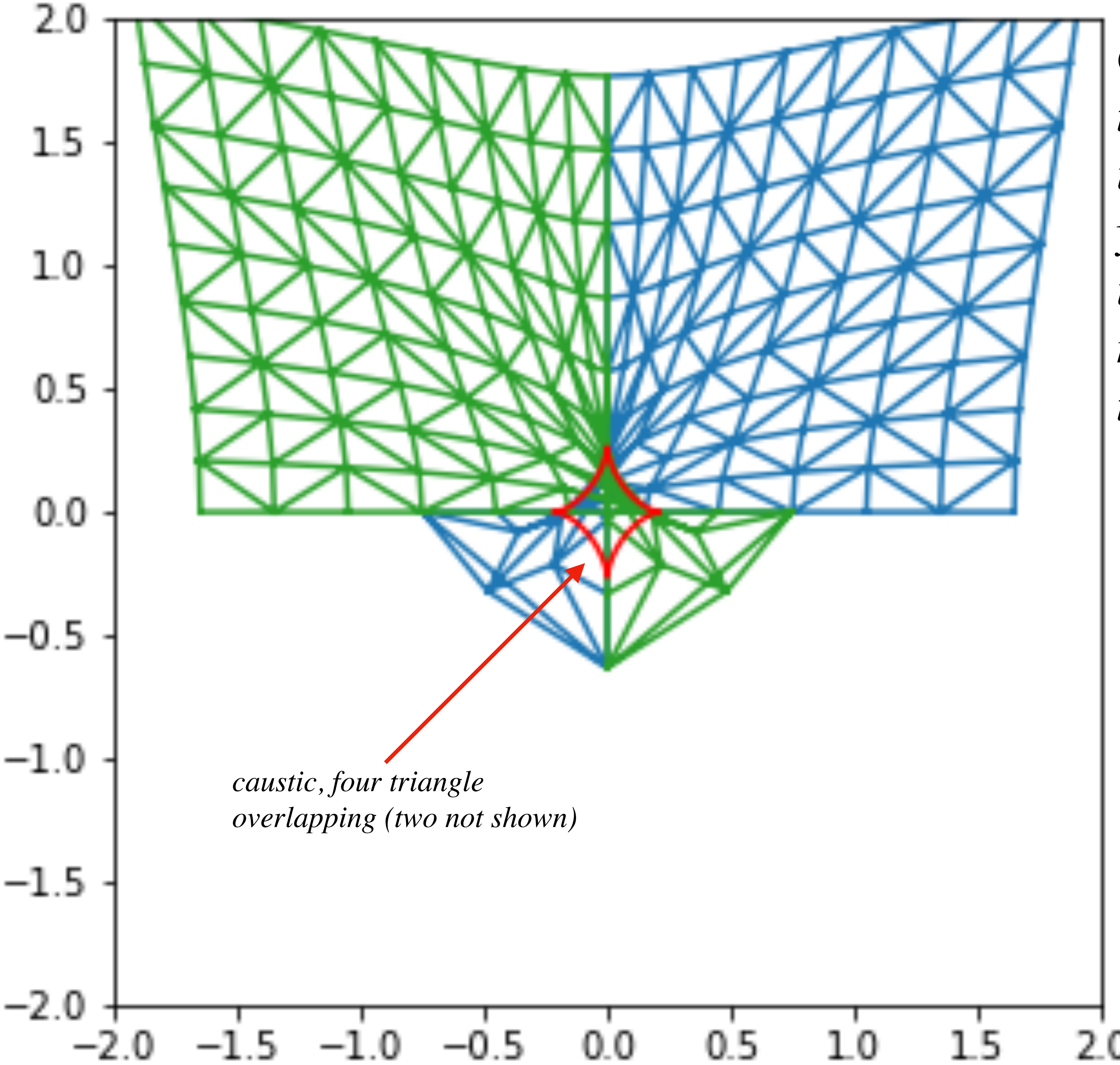

Going back to the triangle on the image plane will tell you where the images are, to the resolution of the tessellation.

DELAUNAY TESSELLATION

Tessellation of image plane.

Divide image plane into triangles.

Find the source position of each vertex point by adding the deflection.

Find which triangle the source is in.

Since the triangle will overlap, the source will be in more than one triangle.

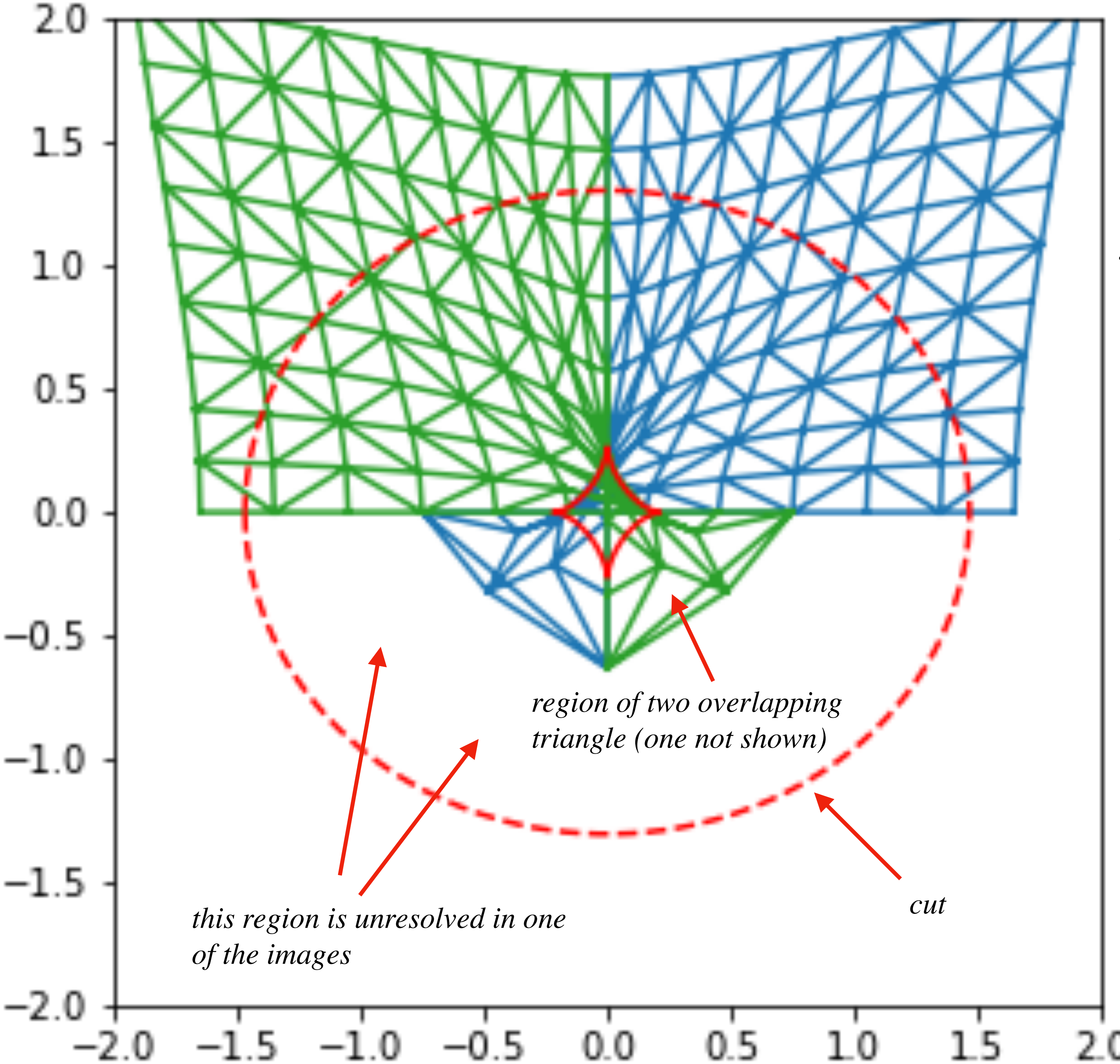

Going back to the triangle on the image plane will tell you where the images are, to the resolution of the tessellation.

Low magnification images can be lost or spurious included.

DELAUNAY TESSELLATION

Tessellation of image plane.

Divide image plane into triangles.

Find the source position of each vertex point by adding the deflection.

Find which triangle the source is in.

Since the triangle will overlap, the source will be in more than one triangle.

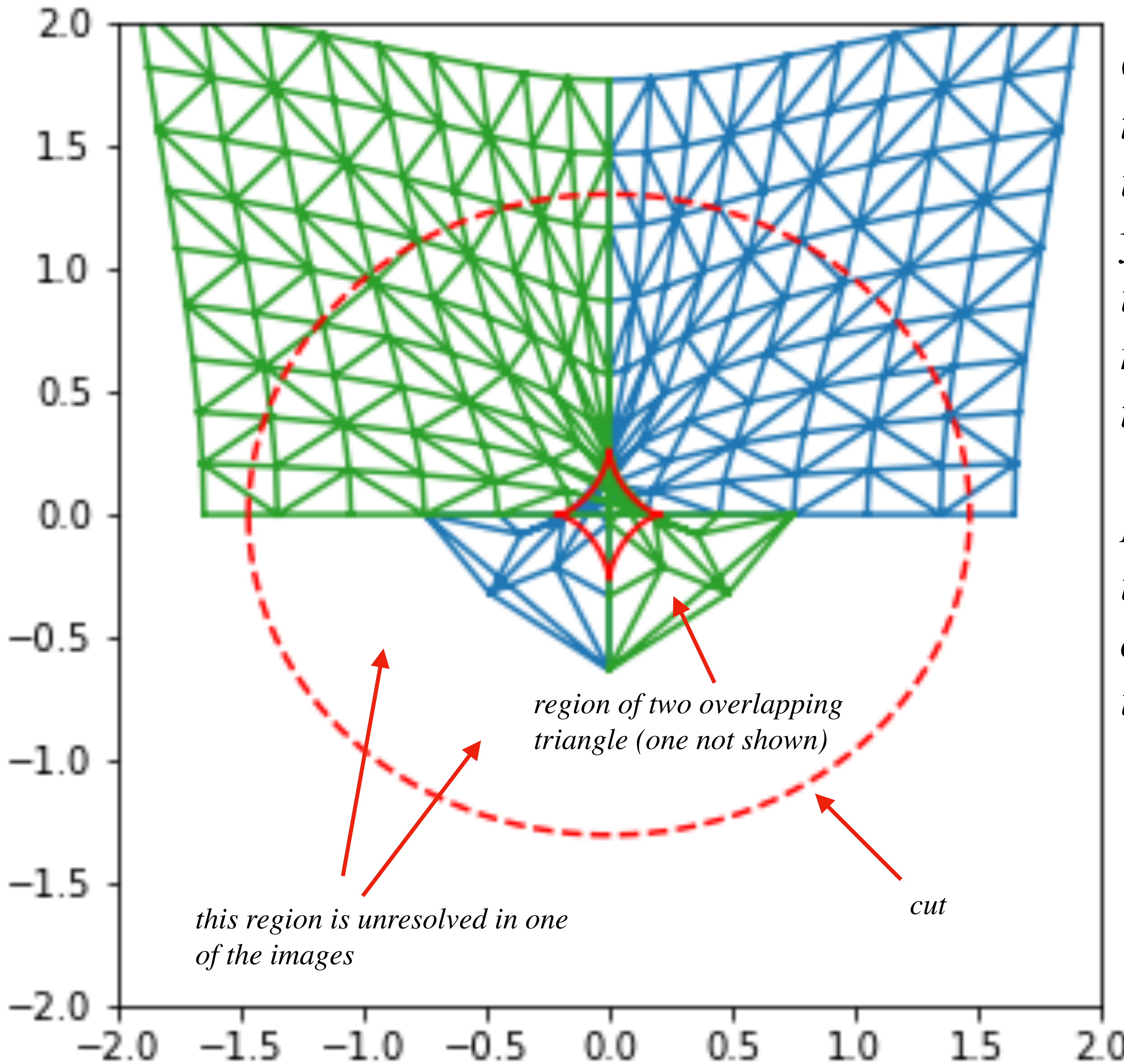

Going back to the triangle on the image plane will tell you where the images are, to the resolution of the tessellation.

Low magnification images can be lost or spurious included.

DELAUNAY TESSELLATION

Tessellation of image plane.

Divide image plane into triangles.

Find the source position of each vertex point by adding the deflection.

Find which triangle the source is in.

Since the triangle will overlap, the source will be in more than one triangle.

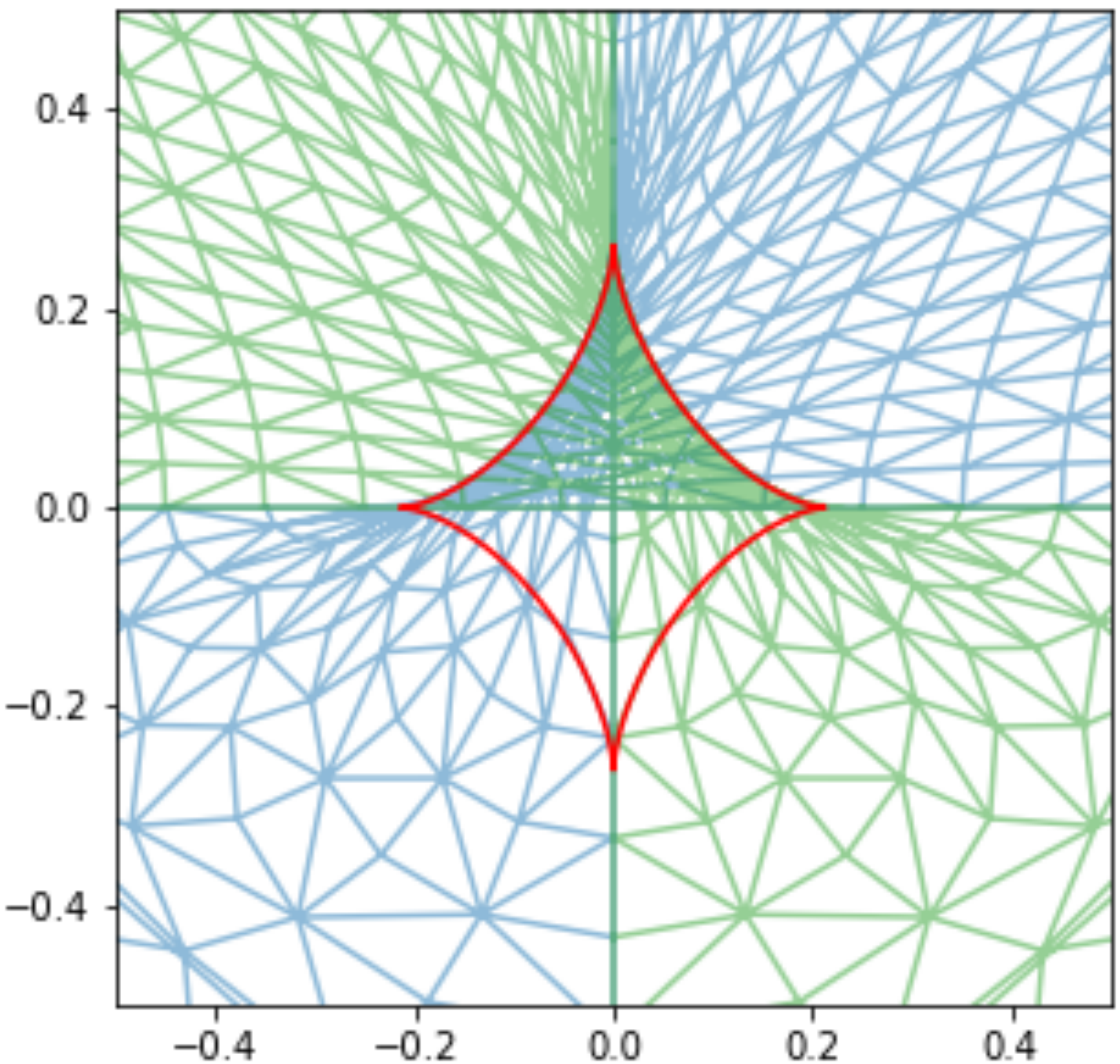

Going back to the triangle on the image plane will tell you where the images are, to the resolution of the tessellation.

Low magnification images can be lost or spurious included.

DELAUNAY TESSELLATION

Points on the source plane from the tessellation of the image plane.

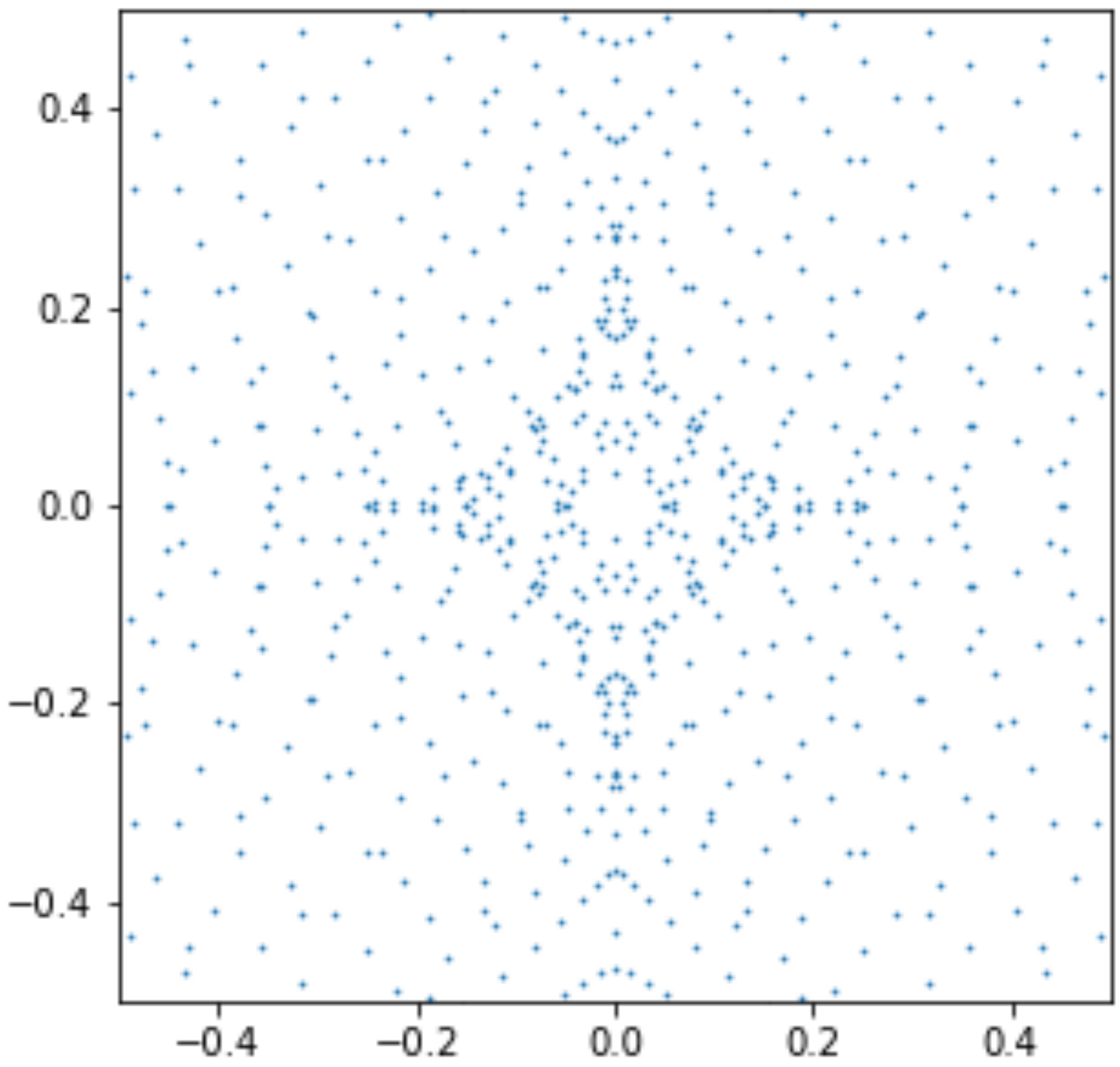

DELAUNAY TESSELLATION

Delaunay tessellation of the source plane.

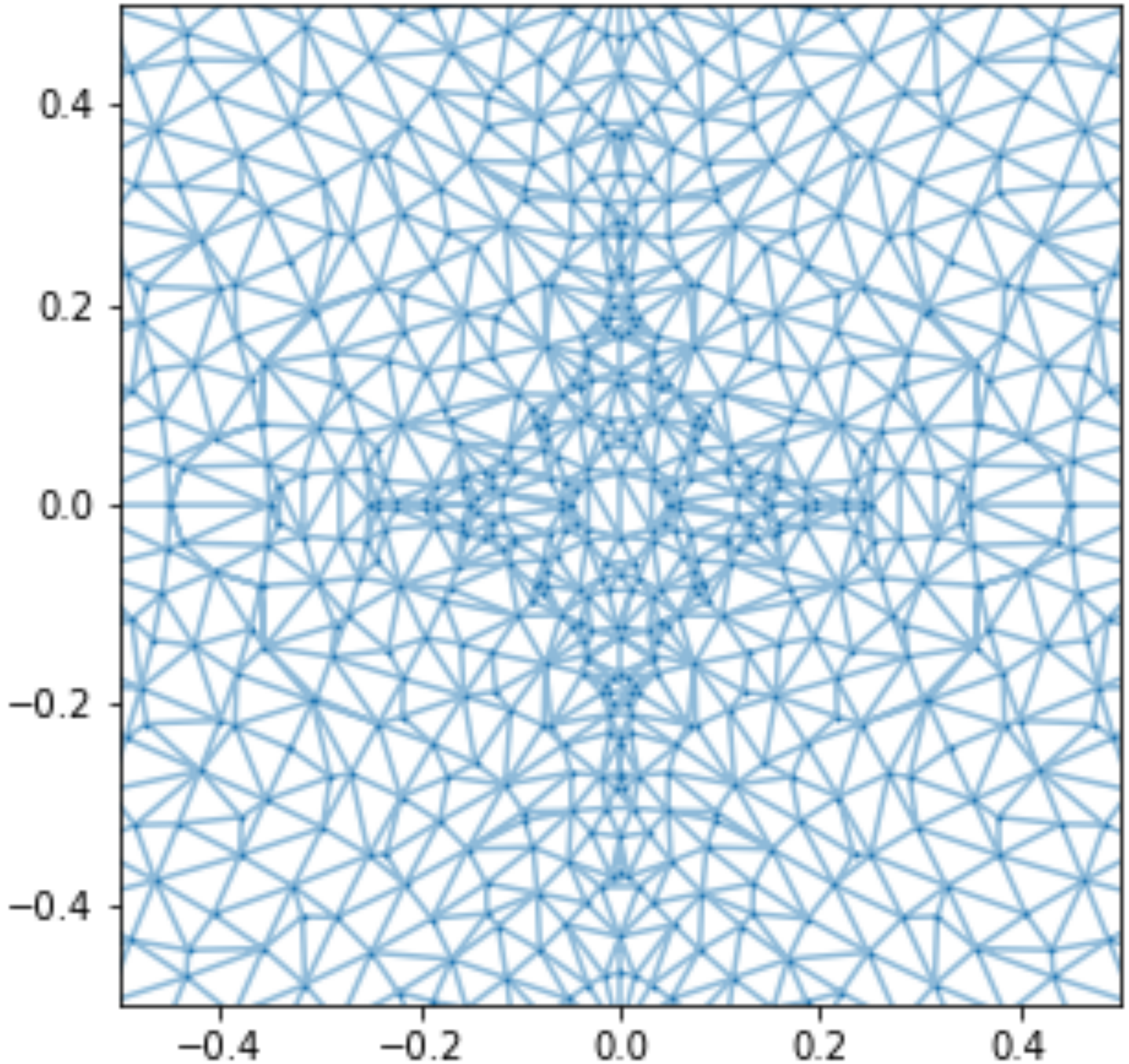

These triangles can be used as pixels for the source reconstruction.

DELAUNAY TESSELLATION

From Massimiliano Zago's thesis

Einstein ring located in a galaxy cluster MACSJ1206.

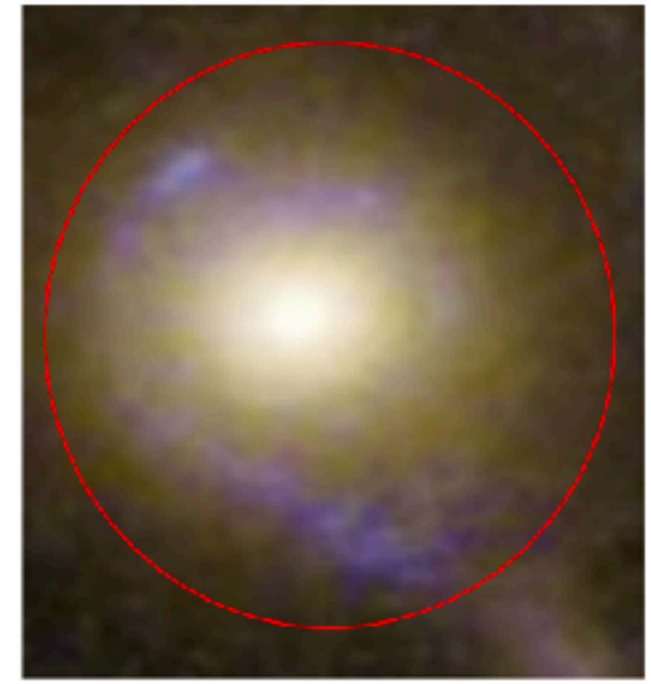

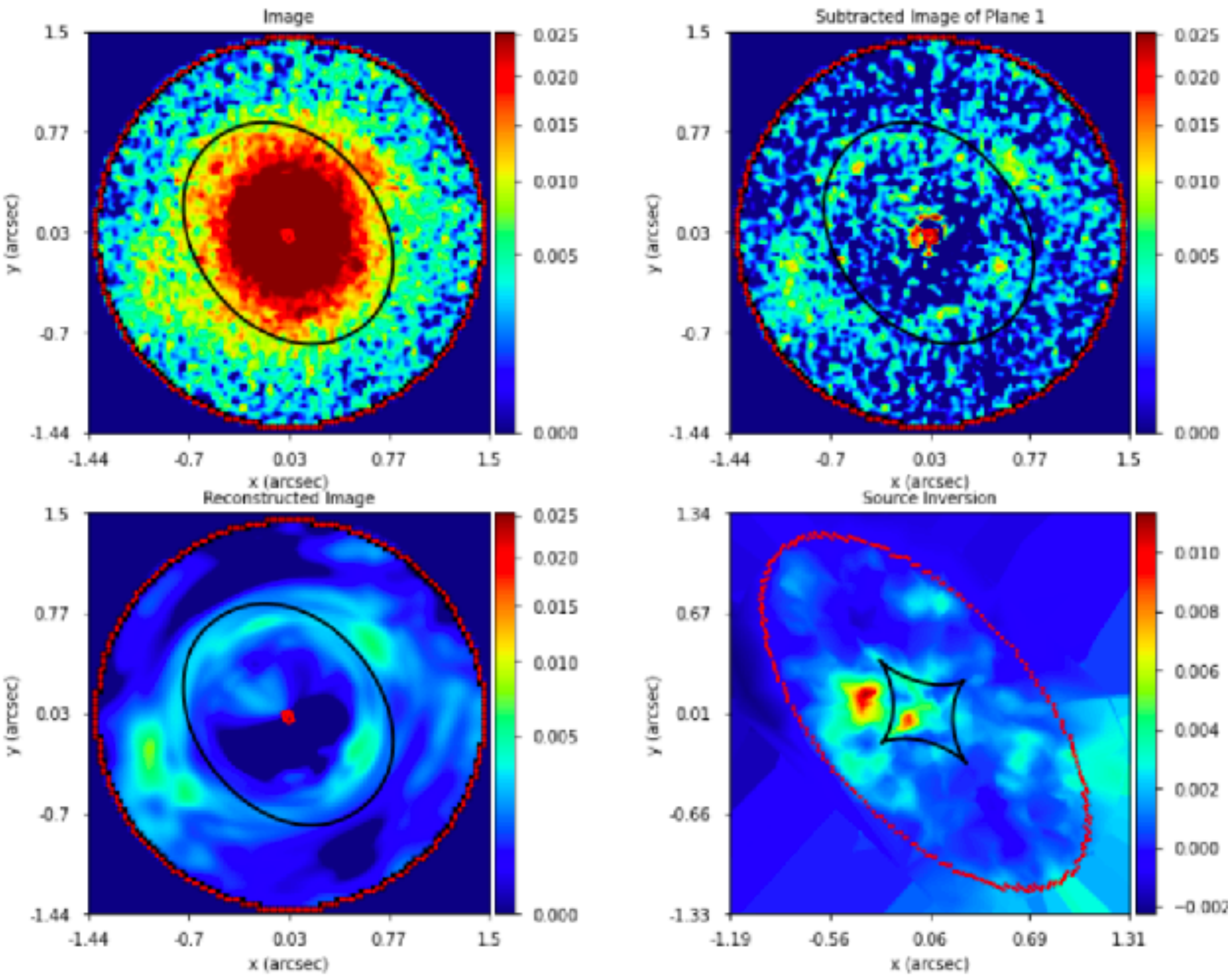

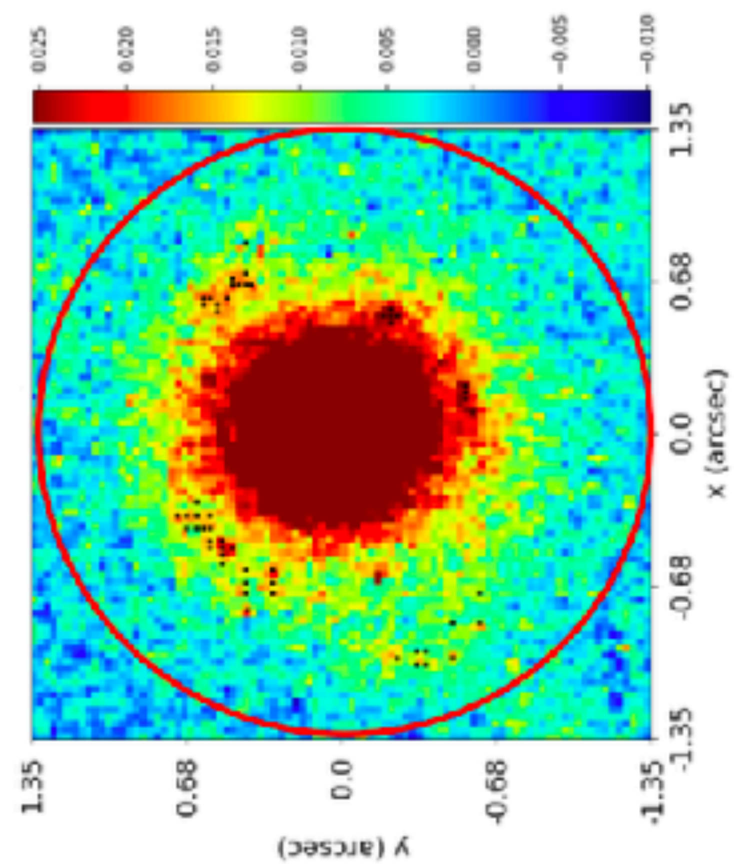

DELAUNAY TESSELLATION

From Massimiliano Zago's thesis

The vertices of the Delaunay tessellation on the source plane.